Contrast-Enhanced Magnetic Resonance Angiography

Julie V. Vasile, MD[a,b,c,*], Tiffany M. Newman, MD[d], Martin R. Prince, MD, PhD[d], David G. Rusch, MD[d,e], David T. Greenspun, MD[a,c], Robert J. Allen, MD[a,c], Joshua L. Levine, MD[a,c]

KEYWORDS

- Autologous perforator flap breast reconstruction
- Magnetic resonance angiography • Imaging • DIEP flap
- SIEA flap • Gluteal artery perforator • TUG flap

Preoperative anatomic imaging of vasculature markedly enhances the ability of a surgeon to devise a surgical strategy before going to the operating room. Before the era of preoperative perforator imaging, a surgeon had little knowledge of an individual patient's vascular anatomy until surgery was well under way. As a result, perforator selection could be a tedious decision process that occurred in the operating room at the expense of operating time and general anesthetic requirement.

The authors' favored modality for preoperative imaging has changed as technology has advanced. Initially only a hand-held Doppler ultrasound was used. A Doppler ultrasound is portable and simple to use, but cannot differentiate perforating vessels from superficial and deep axial vessels or robust perforators from miniscule ones, accurately locate perforators that do not exit perpendicular from the fascia, or provide information on the anatomic course of a vessel.[1,2] By comparison, color Duplex sonography provides more detailed information about the anatomy of the vessels, but requires highly trained technicians with knowledge of perforator anatomy and is time consuming.[2] The technique's most crucial drawback is an inability to produce anatomic images in a format that a surgeon can easily and independently view. As a result, the authors do not use this modality for imaging perforator flaps in their patients.

Computed tomographic angiography (CTA) is a modality that can demonstrate vessel anatomy, assess vessel caliber, accurately locate perforators, and produce anatomic images in a format that a surgeon can easily and independently view. Although CTA can be performed quickly in as little as 15 minutes,[1,2] patients must be exposed to ionizing radiation. Recent articles in the medical literature and lay press warn that physicians may be exposing patients to excessive and potentially unnecessary radiation, and question the long-term effects of such exposure.[3,4] Patients with breast cancer often have a heightened concern for any factor that can potentially increase the risk of developing a second cancer and may perceive the risks of radiation exposure

Disclosure: Dr Prince has patent agreements with GE, Siemens, Phillips, Hitachi, Toshiba, Bracco, Bayer, Epix, Lantheus, Mallinckrodt, Medrad, Nemoto, and Topspins.

[a] Department of Plastic Surgery, New York Eye and Ear Infirmary, 310 East 14th Street, New York, NY 10003, USA
[b] Department of Surgery, Stamford Hospital, 30 Shelburne Road, Stamford, CT 06902, USA
[c] Center for Microsurgical Breast Reconstruction, 1776 Broadway, Suite 1200, New York, NY 10019, USA
[d] Department of Radiology, Weil Cornell Imaging at New York Presbyterian Hospital, Weil Cornell and Columbia University, 416 East 55th Street, New York, NY 10022, USA
[e] Department of Radiology, White Plains Hospital, 41 East Post Road, White Plains, NY 10461, USA
* Corresponding author. 1290 Summer Street, Suite 3200, Stamford, CT 06905.
E-mail address: jvasilemd@gmail.com

Clin Plastic Surg 38 (2011) 263–275
doi:10.1016/j.cps.2011.03.008

even more negatively. A subset of patients with breast cancer gene (BRCA) mutations, which confer an increased risk of developing both breast and ovarian cancer, are especially concerned about receiving radiation to the abdomen. Furthermore, iodinated contrast for CTA has been associated with small, but real risks of anaphylaxis and nephrotoxicity.[5,6]

The dose of radiation from one chest radiograph (0.1 millisieverts [mSv]) is relatively low and is approximately equivalent to the dose of environmental radiation one receives by virtue of living on earth for 10 days.[7] By comparison, a computed tomography (CT) scan of the abdomen delivers 6 to 10 mSv of radiation, which is approximately equivalent to 3 years of environmental radiation.[1,3,7] Controversy lies in the amount of radiation needed for cancer induction, but experts agree that unnecessary exposure to ionizing radiation should be avoided. Frequently the diagnostic utility of CT outweighs the uncertain, low risk of cancer induction.[8] However, the authors believe that alternative methods of vascular imaging should be employed whenever possible, and this led them to consider MRA (magnetic resonance angiography) as an imaging modality.

Magnetic resonance imaging (MRI) works by using a magnetic field to uniformly align the spin of hydrogen atoms in tissue. The subsequent application of a radiofrequency pulse results in release of energy as hydrogen atoms return to their relaxed state. MRI coils detect the released energy, and computer software processes the data into anatomic images. Exposure to a magnetic field or radiofrequency pulse with MRI has not been linked to the development of cancer.[9] A paramagnetic contrast agent (gadolinium-containing) is injected to enhance vessels. Because MRI does not use radiation, multiple series of images can be obtained. Vessels usually are first imaged in the arterial phase, and subsequently the arterial/venous phase for visualization of the artery and vein together. Additional series of images are acquired to view the vasculature in multiple planes: axial, coronal, and sagittal.

Gadolinium-containing contrast agents used for MRA have several distinct advantages over iodinated contrast agents used for CTA. The incidence of an acute allergic reaction to iodinated contrast is 3%, which is orders of magnitude higher than the 0.07% incidence of allergic reaction to gadolinium contrast.[5,10] Furthermore, unlike gadolinium contrast agents, iodinated CT contrast agents can induce renal insufficiency even in patients with normal renal function.[6,11]

Gadolinium contrast agents can potentially induce nephrogenic systemic fibrosis (NSF), also called nephrogenic fibrosing dermopathy. However, reports of NSF have been limited to patients with impaired renal function.[12–14] Patients with an acute kidney injury or chronic severe renal disease (glomerular filtration rate <30 mL/min/1.73 m^2) are considered most at risk.[12] NSF is a very rare disease, with about 330 cases reported worldwide.[13,14] Although patients undergoing elective microsurgical free flap are generally healthy and thus are not at significant risk for developing NSF, a creatinine level is drawn preoperatively in patients with a history of hypertension, diabetes, renal disease, or any other indication that renal function may be impaired.

Disadvantages of MRA are contraindication to use with a cardiac pacemaker or in very claustrophobic patients. However, none of the authors' patients have been excluded from MRA imaging because of these factors. Continuing advances in MRA have decreased the procedure time for a single donor site to as little as 20 minutes and have decreased the actual acquisition scan time to 20 seconds.[15,16]

MRA is currently the favored modality for preoperative imaging because the authors have found the accuracy to be on par with CTA. With their first MRA protocol developed in 2006, in 50 abdominal flaps, the authors found that the location of the perforating vessel correlated with the intraoperative findings within 1 cm in 100% of the flaps, the relative size (ie, comparing size of one vessel to another for the same patient) of the perforators visualized on MRA correlated with the intraoperative findings in 100% of the flaps, all relatively large perforators visualized on MRA were found at surgery (0% false positive), and intraoperative perforators of significant size were visualized on MRA in 96% of the flaps (4% false negative).[17] By comparison, a study using preoperative CTA on 36 patients found 0% false-positive and 0% false-negative results.[1] Another study using preoperative CTA in 42 patients found one false-positive and one false-negative result.[18] The 2 false-negative results in the authors' original study were due to inadequate visualization of lateral row perforators secondary to signal interference from the thigh and buttock fat.

METHODS

Refinements in the authors' MRA protocol were made in 2008.[17,19,20] The switch was made to a 1.5-T scanner to eliminate inhomogeneous fat suppression associated with a 3-T magnet, for improved visualization of lateral row perforators. In addition, gadobenate dimeglumine (Bracco, Princeton, NJ, USA), a gadolinium-based contrast agent that binds to albumin and has a longer half-life in the bloodstream, was used to extend the craniocaudal field of view. Furthermore, the authors

took advantage of the lack of radiation exposure to do serial image acquisitions with a patient in the prone and then supine position. The result of these modifications is that abdominal, gluteal, and upper thigh perforators can be visualized in one study. Also, 3-dimensional (3D) reconstruction was used to view the vessels on surface-rendered images for improved understanding of perforator location.

First, patients were scanned in the prone position because the quality of the images of the abdominal wall perforators is superior to those obtained in the supine position. Respiratory motion is reduced in the prone position and motion artifact is minimized, which enhances abdominal perforator assessment. Fascia is a stable structure in the abdomen, and the location of the abdominal perforators in reference to the base of the umbilical stalk is not affected by the prone position. By contrast, the curved anatomy of the buttock is greatly distorted in the supine position, and buttock perforator location in reference to the gluteal crease is significantly affected. Finally, patients were scanned in the supine position to estimate abdominal flap volume and reconfirm abdominal perforator location.

MRA images and the associated radiology report were reviewed by the surgeon and an optimal perforator(s) was selected. Intraoperative vessel assessment was compared with vessel assessment on MRA, as described in previous articles.[17,19] Immediately after surgery, surveys were completed by the operating surgeon.

PATIENTS

Thirty-seven consecutive patients were imaged with MRA from August 2008 to June 2009. The inclusion criterion was that all patients referred for breast reconstruction were able to travel to the one radiological center that used the authors' MRA protocol. Patients located in other states who could not travel were excluded. Exclusion criterion was inability to undergo MRA examination (cardiac pacemaker, severe claustrophobia, and severe renal insufficiency), for which no patients were excluded.

RESULTS

Sixty-two abdominal, gluteal, thigh, and lumbar flaps were used for breast reconstruction in 37 patients. **Table 1** illustrates the type of flap and type of perforator used.

The new MRA protocol improved the quality of the images and accuracy of perforator assessment. The relative vessel size (ie, comparing size of one vessel to another for the same patient) on MRA compared with that found at surgery was accurate in all flaps (100%), the predicted perforator location was accurate to within 0.5 cm in all flaps (100%), and there were no false-positive (all relatively large perforators visualized on MRA were found at surgery) and no false-negative results (intraoperative perforators of significant size were all visualized on MRA).

The preoperatively selected vessel was used in all patients except in 2 cases. In the first case, a backup inferior gluteal artery perforator (IGAP) vessel was used instead of a planned deep femoral artery perforator (DFAP) in an inferior buttock flap. The IGAP vessel was identified first intraoperatively by the surgeon, and was of adequate caliber, and thus dissected. In the second case, a second small deep inferior epigastric perforator (DIEP) was added to a preoperatively selected large DIEP because it lined up without necessitating an

Table 1
Type of flap and type of perforator(s) used

Flap Type	Number of Flaps	Single Intramuscular Perforator	Double Intramuscular Perforator	Septocutaneous Vessel
DIEP	48	37	9[a]	2
SIEA	1			
SGAP	5	3		2
LAP	1			1
IGAP	2	2[a]		
DFAP	4			4
TUG without muscle	1			1

Abbreviations: DFAP, deep femoral artery perforator; DIEP, deep inferior epigastric perforator; IGAP, inferior gluteal artery perforator; LAP, lumbar artery perforator; SGAP, superior gluteal artery perforator; SIEA, superficial inferior epigastric artery; TUG, transverse upper gracilis.

[a] All preoperatively selected vessels were used to carry the flap, except in one patient a second small DIEP was added to a large preoperatively selected DIEP, and in a second patient a backup IGAP was used instead of a DFAP.

incision through rectus muscle fibers. The second small DIEP was in retrospect visualized on MRA, but not included in the MRA radiology report because the diameter was less than 1 mm.

The design of abdominal flaps was moved cephalad or caudal to capture the best perforator in 20 of 29 patients (69%). In 20 abdominal flaps, the flap weight estimated from MRA differed from the actual flap weight at surgery by an average of 47 g. MRA determined the design of all buttock flaps (100%). MRA determined the selection of which thigh (ipsilateral or contralateral) was used for a unilateral breast reconstruction.

DISCUSSION ON THE FINER POINTS OF MRA AND PERFORATOR SELECTION

Vessel caliber in conjunction with a centralized location on the flap is the most important factor for optimal perforator selection at every donor site. Caliber measurements are uniformly performed at the point where a vessel exits the

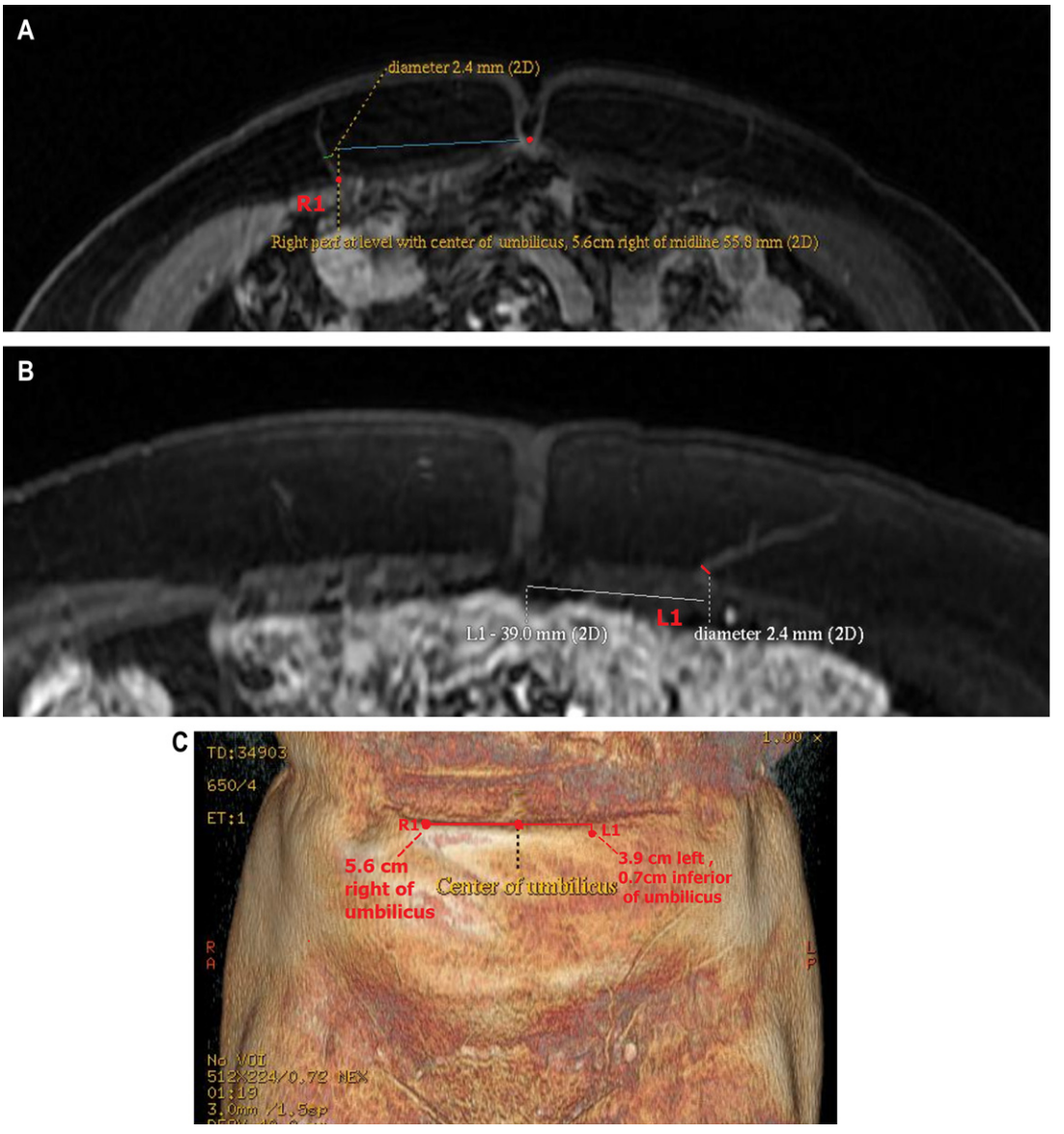

Fig. 1. (*A*) Axial MRA of perforator R1. Location is measured in reference to the base of the center of the umbilical stalk. (*B*) Axial MRA of perforator L1. Diameter is measured at the point where the perforator exits the anterior rectus fascia. (*C*) Surface-rendered 3-dimensional (3D) reconstruction MRA. Location of perforators is in reference to the umbilicus.

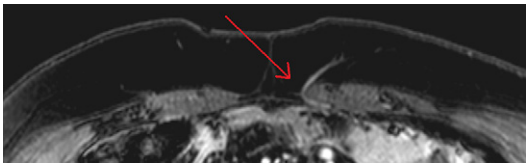

Fig. 2. Axial MRA. Arrow points to septocutaneous perforator. (*From* Greenspun D, Vasile J, Levine JL, et al. Anatomic imaging of abdominal perforator flaps without ionizing radiation: seeing is believing with magnetic resonance imaging angiography. J Reconstr Microsurg 2010;26(1):41; with permission.)

superficial fascia. Location measurements are performed in reference to a landmark at each donor site. Specific considerations regarding each donor site are presented here.

Abdomen

The location of the vessel on exiting the anterior rectus fascia is measured in reference to the center of the base of the umbilical stalk for improved accuracy, as seen in **Fig. 1**. Vessel caliber measurements are also performed just

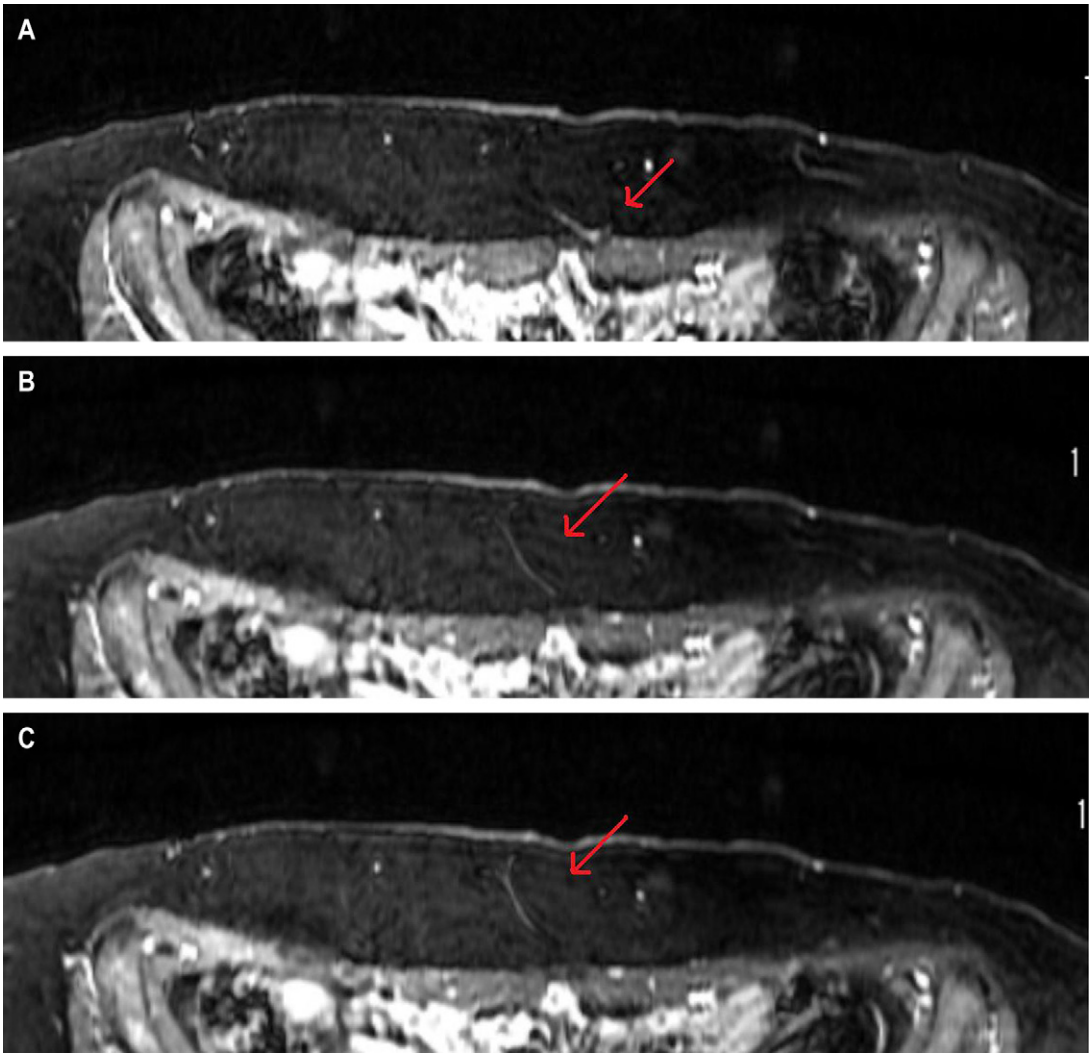

Fig. 3. (*A*) Axial MRA. Arrow points to medial row perforator. (*B*) Axial MRA. Arrow points to arborization of the same perforator crossing the midline. (*C*) Axial MRA. Arrow points to further arborization of the same perforator.

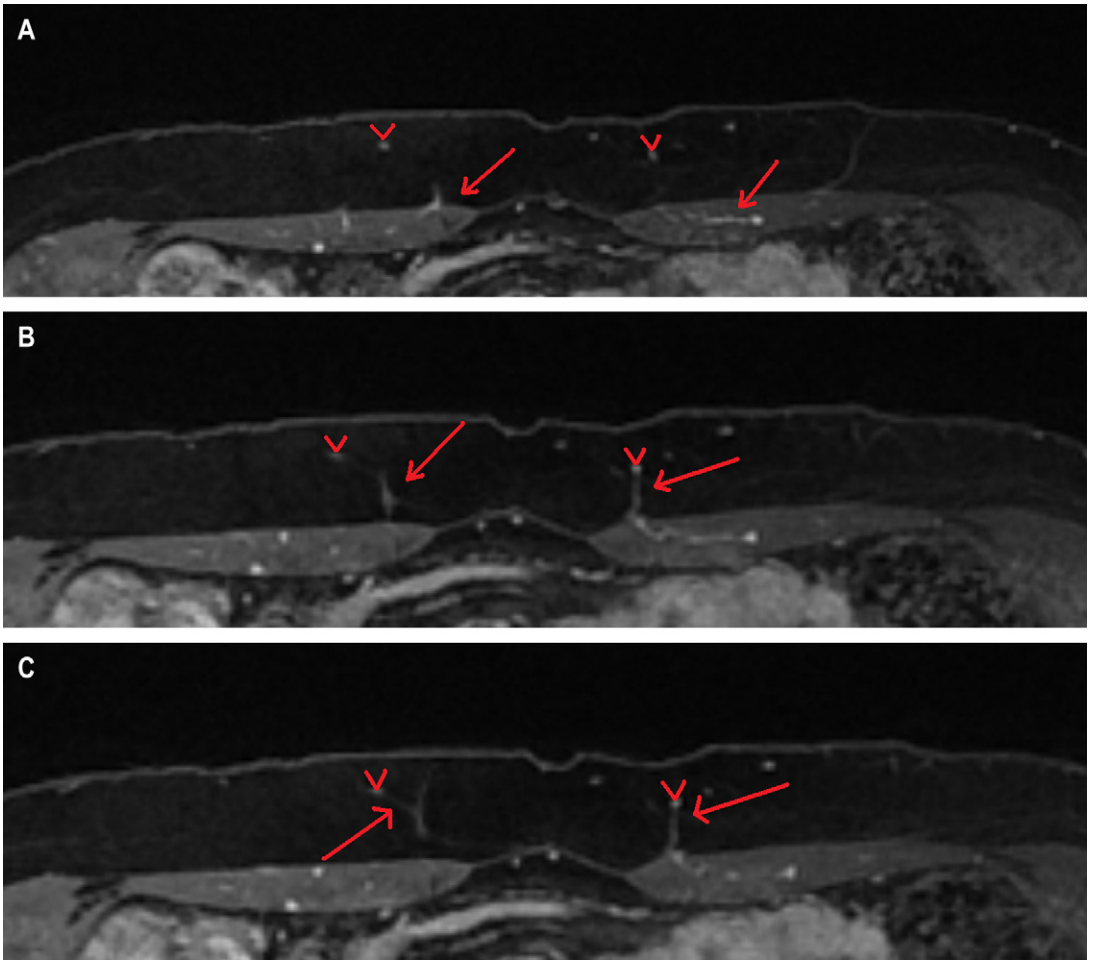

Fig. 4. "V" denotes superficial inferior epigastric vein (SIEV), and arrows point to bilateral deep inferior epigastric perforators (DIEPs). (*A*) Axial MRA. (*B*) Axial MRA. Left DIEP meeting SIEV. (*C*) Axial MRA. Right DIEP branch also meeting SIEV.

above the anterior rectus fascia level. An intramuscular course length or a septocutaneous course, as seen in **Fig. 2**, can add important information for a surgeon to anticipate a tedious or straightforward dissection. Also, the branching pattern of the vessel in the subcutaneous fat may provide valuable information. In a unilateral reconstruction, it is helpful to see a medial row perforator with branches crossing into the subcutaneous fat on the contralateral abdomen, because zone III is more likely to be well perfused, as seen in **Fig. 3**. In addition, DIEP branches connecting with

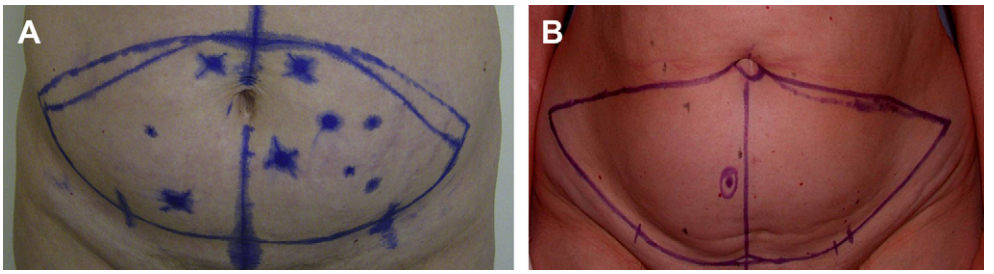

Fig. 5. (*A*) Abdominal flap design shifted cephalad to capture the 2 largest perforators located above the umbilicus. (*B*) Abdominal flap design shifted caudal.

superficial inferior epigastric venous branches may theoretically provide improved venous drainage. An example of a DIEP connecting with a superficial inferior epigastric vein branch is seen in **Fig. 4**.[21]

The detailed information on vasculature provided by MRA influences flap design. As a result of imaging, the design of abdominal flaps was moved cephalad or caudal to capture the best perforator in 20 of 29 patients (69%). Pictures of two different flap designs are seen in **Fig. 5**.

Helpful images that a radiologist can add to the study are coronal images, which best show the branching pattern of the deep inferior epigastric system, as seen in **Fig. 6**. Also, 3D reconstructed images are useful in examining for a common origin of the superficial inferior epigastric artery with the superficial circumflex iliac artery, as seen in **Fig. 7**. However, a superficial inferior epigastric artery was rarely used because a DIEP with adequate caliber and location was usually found. In the authors' study, 48 DIEP (98%) and 1 superficial inferior epigastric artery (SIEA) (2%) vessels were used. In the one case that a SIEA was used, a contralateral SIEA was added to augment perfusion in a unilateral DIEP flap breast reconstruction, in which zone III and a portion of zone IV of the abdomen required additional perfusion.

Volume-rendered 3D reconstructions can be performed by a radiologist to add important information on the projected abdominal flap weight, as seen in **Fig. 8**. First, a radiologist has to be trained in the typical markings and dimensions of an abdominal flap to increase accuracy. In 20 abdominal flaps, the flap weight estimated from MRA differed from the actual flap weight at surgery by an average of 47 g.[20,22] The weight difference can be attributed to several causes: the mean density of fat (0.92) was used in the volume calculation, but the abdominal flap also contains skin and vessels; the actual flap dimensions marked by a surgeon will differ from those made by a radiologist; beveling of extra subcutaneous fat outside the marked dimension during surgery was sometimes performed; and extra tissue was taken outside the marked dimension to harvest an inguinal lymph node with 2 DIEP flaps for lymph node transfer in 2 patients with mastectomy and upper extremity lymphedema.

Fig. 6. Coronal MRA. The branching pattern of the deep inferior epigastric system is visualized. Arrows point to bifurcation of deep inferior epigastric vessels bilaterally.

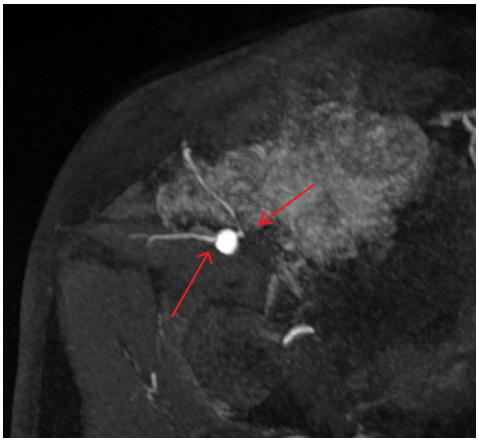

Fig. 7. 3D Reconstruction MRA. Arrows point to separate origin of the superficial inferior epigastric artery and superficial circumflex iliac artery. (*From* Greenspun D, Vasile J, Levine JL, et al. Anatomic imaging of abdominal perforator flaps without ionizing radiation: seeing is believing with magnetic resonance imaging angiography. J Reconstr Microsurg 2010; 26(1):43; with permission.)

Buttock

A photograph of the marked top of the gluteal crease is included in the radiology report for increased accuracy, as seen in **Fig. 9**. The location of the vessel on exiting the superficial fascia is measured in reference to the top of the gluteal crease along the curved skin contour of the buttock with the patient in the prone position for increased accuracy, as seen in **Fig. 10**. Surface-rendered 3D reconstruction is invaluable to the surgeon for location of perforators because of the curved contour of the buttock.

The placement of the buttock flap skin paddle is also significantly influenced by optimal perforator

Fig. 8. Volume-rendered 3D reconstruction MRA. Abdominal flap volume measured by the radiologist.

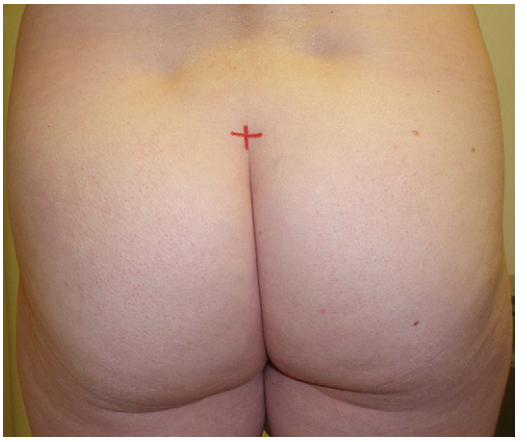

Fig. 9. Top of gluteal crease is the reference point marked by the radiologist.

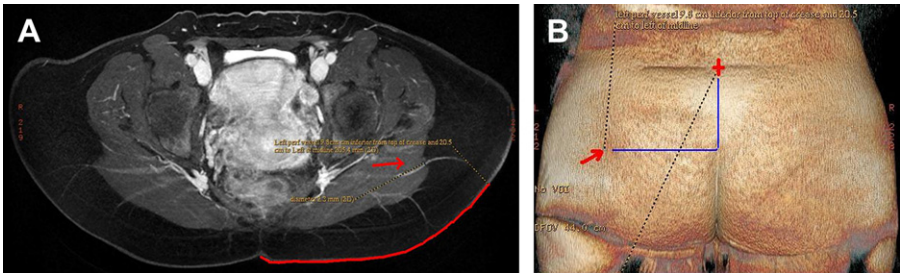

Fig. 10. (*A*) Axial MRA. Gluteal perforator location is measured along the curved skin surface. (*B*) Surface-rendered 3D reconstruction MRA. Same perforator located on the buttock, in reference to top of gluteal crease. (*From* Vasile JV, Newman T, Rusch DG, et al. Anatomic imaging of gluteal perforator flaps without ionizing radiation: seeing is believing with magnetic resonance angiography. J Reconstr Microsurg 2010;26(1):48; with permission.)

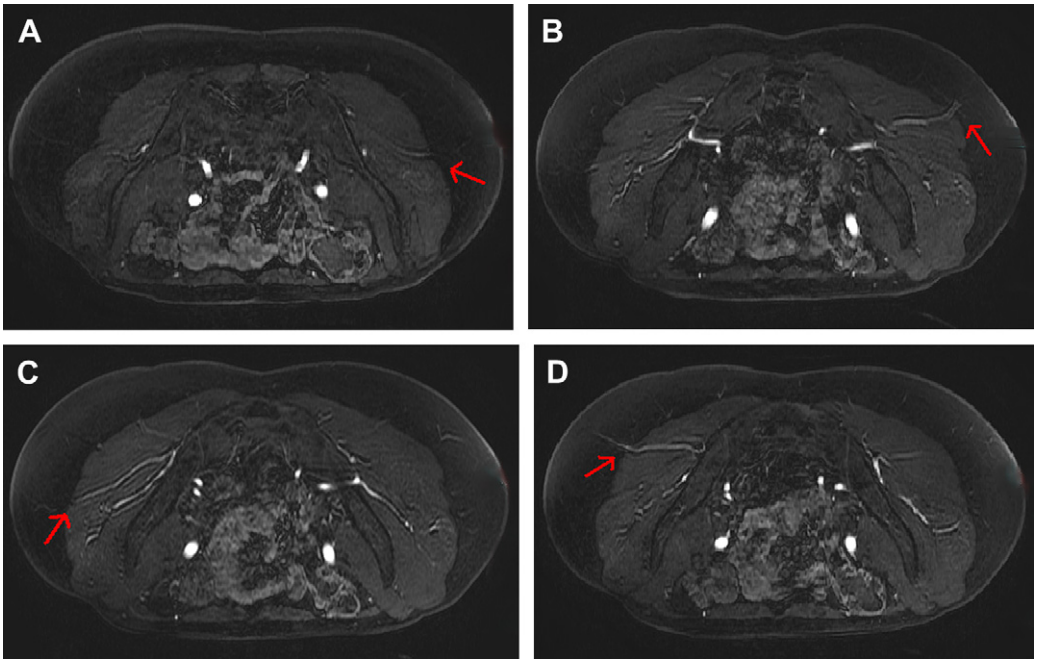

Fig. 11. Arrows point to laterally and cephalad located perforators on the same patient. (*A*) Axial MRA. Right septocutaneous superior gluteal artery perforator (SGAP). (*B*) Axial MRA. Right intramuscular double branching SGAP. (*C*) Axial MRA. Left septocutaneous SGAP. (*D*) Axial MRA. Left intramuscular SGAP. (*From* Vasile JV, Newman T, Rusch DG, et al. Anatomic imaging of gluteal perforator flaps without ionizing radiation: seeing is believing with magnetic resonance angiography. J Reconstr Microsurg 2010;26(1):53; with permission.)

location. The goal is to design a flap that incorporates the optimal perforator and a back up option. Because there are usually many large-caliber perforator options in the buttock, vessel location is an important determining factor in selecting the optimal vessel. Laterally positioned perforators will result in more lateral flaps that may spare the central aesthetic unit in superior buttock flaps or the medial cushioning fat in lower buttock flaps. In bilateral flaps, an attempt is made to design flaps that will result in symmetric scars. Examples are shown in **Figs. 11 to 14**.

A benefit of precise knowledge of a patient's vascular anatomy is the ability and confidence to design flaps based on vessels not previously used. **Figs. 13** and **14** illustrate an MRA of a DFAP, which can be advantageous because it usually results in a more laterally and caudally positioned lower buttock flap. In addition, DFAPs are usually septocutaneous after piercing the adductor magnus muscle proximally.[19] In addition, **Fig. 15** illustrates the MRA and flap design of a lumbar artery perforator (LAP) flap, which can be positioned more superiorly to better spare the central aesthetic unit in the buttock and is usually septocutaneous.

Thigh

The design of a medial upper thigh (transverse upper gracilis; TUG) flap is usually fairly standard, and designed to incorporate branches coursing

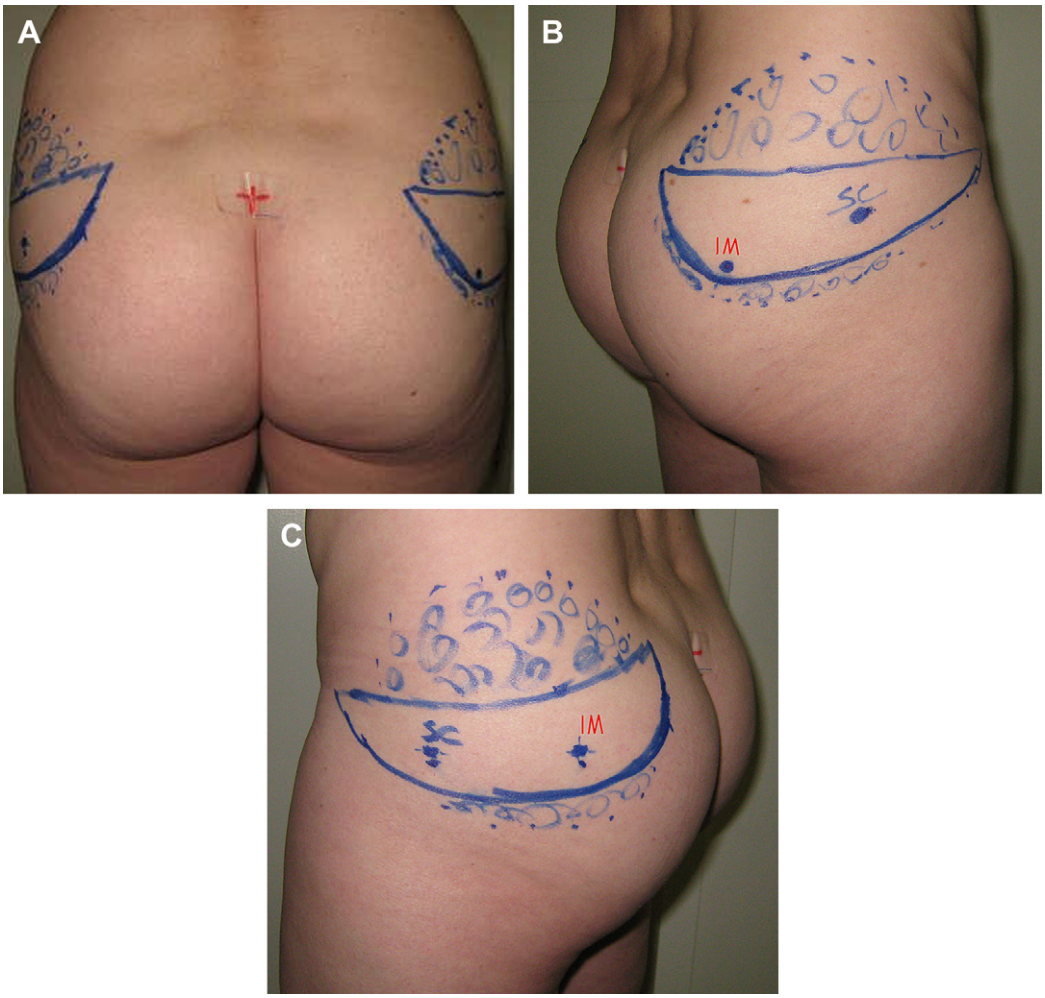

Fig. 12. Flaps designed to incorporate the septocutaneous and backup intramuscular SGAP shown in **Fig. 11**. Septocutaneous perforator is marked "SC" and intramuscular perforator is marked "IM." Planned harvest of subcutaneous fat outside the flap design is marked. (*A*) Posterior buttock. Note that flaps are positioned laterally to spare central aesthetic unit. (*B*) Right oblique buttock. (*C*) Left oblique buttock. (*From* Vasile JV, Newman T, Rusch DG, et al. Anatomic imaging of gluteal perforator flaps without ionizing radiation: seeing is believing with magnetic resonance angiography. J Reconstr Microsurg 2010;26(1):54; with permission.)

through the gracilis muscle from the medial circumflex femoral artery, located 10 cm caudal to the pubic tubercle. Usually a portion of the gracilis muscle is harvested in a TUG flap. However, upper thigh imaging can yield very useful information that can influence surgical planning. **Fig. 16** illustrates an MRA of a septocutaneous perforator from the medial circumflex femoral artery in a patient undergoing a unilateral breast reconstruction. Harvest of this septocutaneous vessel resulted in complete sparing of the gracilis muscle and determined the donor site (ie, which thigh to use for reconstruction). Sometimes a perforator from the medial circumflex femoral artery is large and can be dissected between the gracilis muscle fibers to spare harvesting the gracilis muscle. Moreover, a branch from the superficial femoral artery or deep femoral artery can be used to harvest the same upper thigh tissue and also spare the gracilis muscle.

CURRENT MRA PROTOCOL

In January 2010, the authors switched to a blood pool contrast agent, gadofosveset trisodium (Lantheus Medical Imaging, North Billerica, MA, USA). Gadofosveset trisodium (Ablavar) reversibly binds to albumin with a higher (approximately 90%) binding fraction and effectively stays intravascular for almost an hour (redistribution half-life = 48 minutes) to allow for excellent-quality images over an expanded examination window.[23,24] Increased imaging quality of the visualization of perforators was immediately noticed, especially through muscle, which can be helpful in determining the intramuscular course.

At the same time the authors switched contrast agents, they came to the realization that the combined arterial venous phase is more useful in selecting the optimal perforator because a perforating artery is paired with a vein, and together they are more easily identified when there is simultaneous enhancement of both vessels.

The most current MRA protocol is as follows. MRA is performed on a long-bore, self-shielded 1.5-T scanner (GE Signa 14.0, Waukasha, WI, USA) using an 8-channel phased-array coil. The field of view extends from 3 cm above the umbilicus to the upper thigh and transversely is set to match the width of the patient. Slice thickness is 3 mm with 1.5-mm overlap. Frequency and reduced field of view shim are adjusted to ensure effective fat suppression over the anterior abdominal fat on precontrast imaging. The first acquisition is started 3 seconds after observation of contrast in the suprarenal aorta (SmartPrep). k-Space is mapped sequentially so the absolute

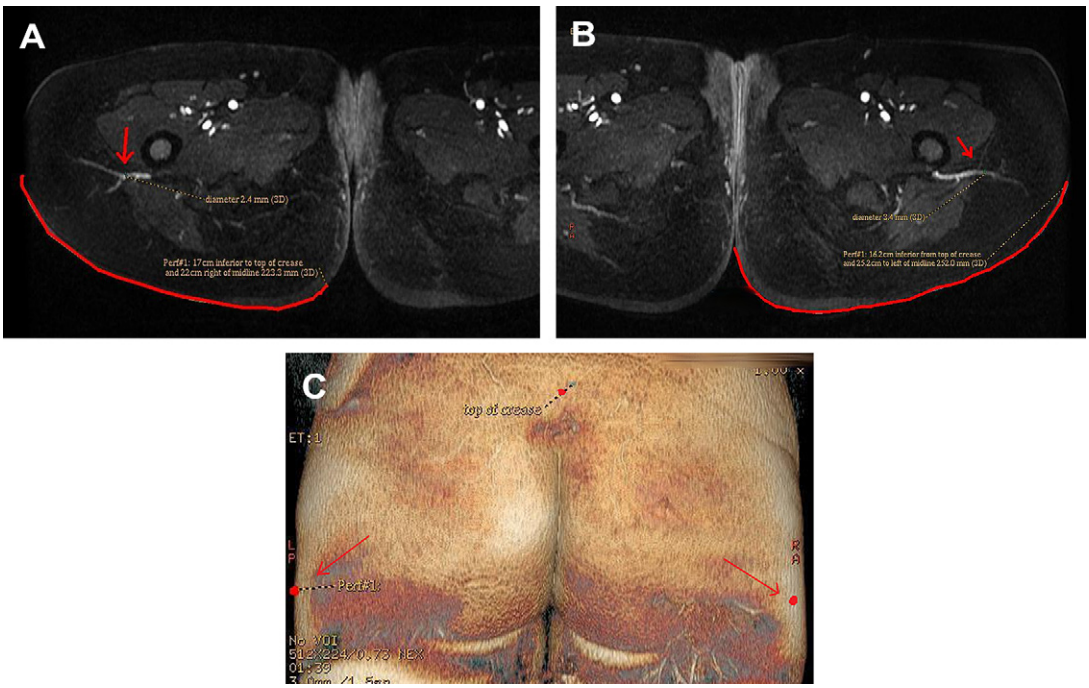

Fig. 13. Arrows point to laterally and caudally located perforators on the same patient. (*A*) Axial MRA. Right septocutaneous deep femoral artery perforator (DFAP). (*B*) Axial MRA. Left septocutaneous DFAP. (*C*) Surface-rendered 3D reconstruction MRA. DFAPs located on buttock skin surface. (*From* Vasile JV, Newman T, Rusch DG, et al. Anatomic imaging of gluteal perforator flaps without ionizing radiation: seeing is believing with magnetic resonance angiography. J Reconstr Microsurg 2010;26(1):49, 50; with permission.)

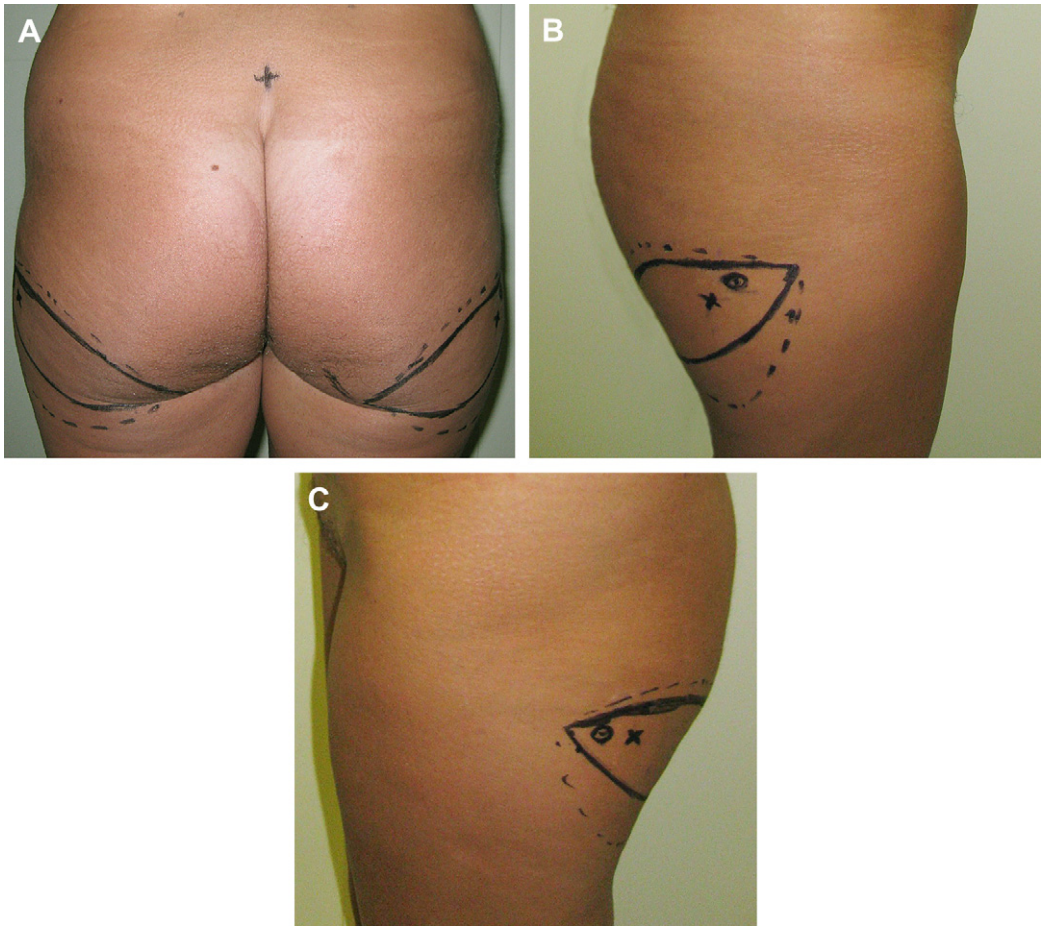

Fig. 14. Flaps designed to incorporate the DFAPs shown in **Fig. 13**. Planned harvest of subcutaneous fat outside the flap is marked with dotted line. (*A*) Posterior buttock. Note that flaps are positioned lateral to spare cushion fat medially. (*B*) Right lateral buttock. (*C*) Left lateral buttock. (*From* Vasile JV, Newman T, Rusch DG, et al. Anatomic imaging of gluteal perforator flaps without ionizing radiation: seeing is believing with magnetic resonance angiography. J Reconstr Microsurg 2010;26(1):51; with permission.)

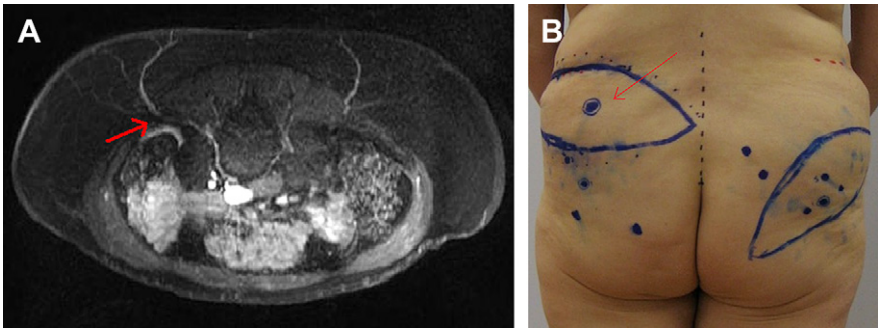

Fig. 15. (*A*) Axial MRA. Arrow points to left lumbar artery perforator (LAP). (*B*) Posterior buttock. Left buttock flap is designed to incorporate LAP (*arrow*). Back up GAP flap was designed, but not used on right buttock. (*From* Vasile JV, Newman T, Rusch DG, et al. Anatomic imaging of gluteal perforator flaps without ionizing radiation: seeing is believing with magnetic resonance angiography. J Reconstr Microsurg 2010;26(1):55; with permission.)

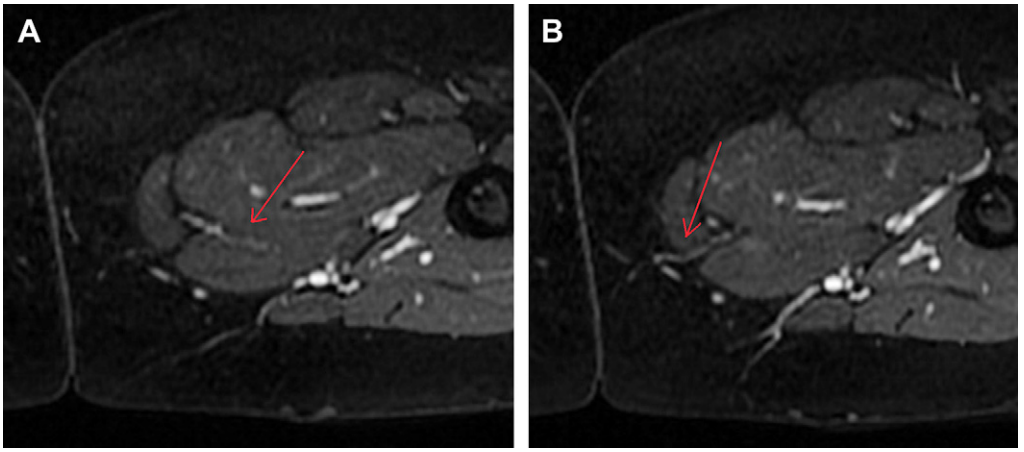

Fig. 16. (*A*) Axial MRA. Arrow points to medial circumflex artery perforator. (*B*) Axial MRA. Arrow points to septocutaneous course of perforator around gracilis muscle.

center of k-space is collected in the middle of the scan (20 seconds after contrast detection). Length of breath-hold is 30 to 35 seconds per acquisition. Repetition time/echo time/flip = 4/1.9/15°. Matrix = 512 × 192–256. Bandwidth = 125 kHz. The injection consists of 10 mL of gadofosveset trisodium at 1 mL/s followed by 20 mL of normal saline. The patient is placed in the prone position for the following sequences: axial and coronal T2-weighted single-shot fast spin echo (SSFSE) images, axial high-resolution 3D liver accelerated volume acquisition (LAVA) pre/during/postdynamic injection of contrast, and postcontrast coronal and sagittal LAVA. The patient is positioned supine for axial high-resolution LAVA. Images are postprocessed on an Advantage Workstation.

This current MRA protocol allows multiple studies in one, and imaging time averages 40 minutes. A patient who unexpectedly is not a candidate for an abdominal perforator flap based on imaging findings, or suddenly changes her preference of donor site, or has a flap failure and requires another perforator flap reconstruction, does not require further studies.

SUMMARY

The tremendous anatomic variability in the vascular system can make perforator flap breast reconstruction challenging for surgeons at all experience levels. Accurate preoperative anatomic vascular imaging enables optimal perforator selection and improves flap design. Shifting the brunt of the perforator selection process preoperatively improves operating efficiency, which can result in reduced operating time, reduced general anesthesia requirements, and potentially increased flap success.[17,25] The authors consider MRA to be the preoperative method of choice, due to the absence of radiation exposure or iodinated contrast agents and the ability for serial imaging acquisitions to visualize multiple donor site vasculature in one study.

REFERENCES

1. Masia J, Clavero JA, Larranaga JR, et al. Multidetector-row computed tomography in the planning of abdominal perforator flaps. J Plast Reconstr Aesthet Surg 2006;59(6):594–9.
2. Rozen WM, Phillips TJ, Ashton MW, et al. Preoperative imaging for DIEA perforator flaps: a comparative study of computed tomographic angiography and Doppler ultrasound. Plast Reconstr Surg 2008; 121(1):9–16.
3. Brenner DJ, Hall EJ. Computed tomography-an increasing source of radiation exposure. N Engl J Med 2007;357(22):2277–84.
4. Stein R. Too much of a good thing? The growing use of CT scans fuel medical concerns regarding radiation exposure. The Washington Post Newspaper. January 15, 2008.
5. Katayama H, Yamaguchi K, Kozuka T, et al. Adverse reactions to ionic and nonionic contrast media. A report from the Japanese committee on the safety of contrast media. Radiology 1990;175(3):621–8.
6. Parfray P. The clinical epidemiology of contrast-induced nephropathy. Cardiovasc Intervent Radiol 2005;28(Suppl 2):S3–11.
7. Safety in Medical Imaging. American College Radiology Radiological Society North America, Inc. Available at: www.radiologyinfo.org/en/safety/index.cfm?pg=sfty_xray&bhcp=1. Accessed September 27, 2010.
8. Varnholt H. Computed tomography and radiation exposure. N Engl J Med 2008;358(8):852–3.

9. Shellock FG, Crues JV. MR procedures: biologic effects, safety, and patient care. Radiology 2004; 232:635–52.
10. Dillman JR, Ellis JH, Cohan RH, et al. Frequency and severity of acute allergic-like reactions to gadolinium-containing IV contrast media in children and adults. AJR Am J Roentgenol 2007;189:1533–8.
11. Niendorf HP, Alhassan A, Geens VR, et al. Safety review of gadopentetate dimeglumine extended clinical experience after more than five million applications. Invest Radiol 1994;29(Suppl 2):S179–82.
12. FDA drug safety communication: new warnings for using gadolinium-based contrast agents in patients with kidney dysfunction. Available at: http://www.fda.gov/drugs/drugsafety/ucm223966.htm. Accessed September 21, 2010.
13. Cowper SE. Nephrogenic fibrosing dermopathy [ICNSFR Website]. 2001-2009. Available at: http://www.icnsfr.org. Accessed September 22, 2010.
14. Scheinfeld NS, Cowper SE. Nephrogenic fibrosing dermopathy. 2008. Available at: http://www.emedicine.com/derm/topic934.htm. Accessed August 7, 2008.
15. Neil-Dwyer JG, Ludman CN, Schaverien M, et al. Magnetic resonance angiography in preoperative planning of deep inferior epigastric artery perforator flaps. J Plast Reconstr Aesthet Surg 2009; 62:1661–5.
16. Masia J, Kosutic D, Cervelli D, et al. In search of the ideal method in perforator mapping: noncontrast magnetic resonance imaging. J Reconstr Microsurg 2010;26(1):29–35.
17. Greenspun D, Vasile J, Levine JL, et al. Anatomic imaging of abdominal perforator flaps without ionizing radiation: seeing is believing with magnetic resonance imaging angiography. J Reconstr Microsurg 2010;26(1):37–44.
18. Rozen WM, Ashton MW, Stella DL, et al. The accuracy of computed tomographic angiography for mapping the perforators of the deep inferior epigastric artery: a blinded, prospective cohort study. Plast Reconstr Surg 2008;122(4):1003–9.
19. Vasile JV, Newman T, Rusch DG, et al. Anatomic imaging of gluteal perforator flaps without ionizing radiation: seeing is believing with magnetic resonance angiography. J Reconstr Microsurg 2010; 26(1):45–57.
20. Newman TM, Vasile J, Levine JL, et al. Perforator flap magnetic resonance angiography for reconstructive breast surgery: a review of 25 deep inferior epigastric and gluteal perforator artery flap patients. J Magn Reson Imaging 2010;31(5):1176–84.
21. Schaverien MV, Ludman CN, Neil-Dwyer J, et al. Relationship between venous congestion and intra-flap venous anatomy in DIEP flaps using contrast-enhanced magnetic resonance angiography. Plast Reconstr Surg 2010;126(2):385–92.
22. Vasile J, Newman T, Greenspun D. Anatomic vascular imaging of perforator flaps for breast reconstruction: seeing is believing with MRA. Plast Reconstr Surg 2009;124(4S):71.
23. Ersoy H, Jacobs P, Kent CK, et al. Blood pool MR angiography of aortic stent-graft endoleak. AJR Am J Roentgenol 2004;182:1181–6.
24. Klessen C, Hein PA, Huppertz A, et al. First-pass whole-body magnetic resonance angiography (MRA) using the blood-pool contrast medium gadofosveset trisodium: comparison to gadopentetate dimeglumine. Invest Radiol 2007;42:659–64.
25. Casey W, Chew RT, Rebecca AM, et al. Advantages of preoperative computed tomography in deep inferior epigastric artery perforator flap breast reconstruction. Plast Reconstr Surg 2009;123(4): 1148–55.